Observations of GW/TID oscillations in the *F*2 layer at low latitude during high and low solar activity, geomagnetic quiet and disturbed periods

V. Klausner,[1] P. R. Fagundes,[1] Y. Sahai,[1] C. M. Wrasse,[1] V. G. Pillat,[1] and F. Becker-Guedes[1]

Received 3 June 2008; revised 10 November 2008; accepted 26 November 2008; published 21 February 2009.

[1] Ionospheric vertical sounding observations, using a digital ionosonde, are being carried out on a routine basis at Sao Jose dos Campos (23.2°S, 45.9°W; dip latitude 17.6°S, hereafter referred to as SJC), Brazil, located under the southern crest of the equatorial ionization anomaly (EIA), since August 2000. In this paper, we present and discuss the seasonal variation of gravity wave (GW) and traveling ionospheric disturbance (TID) oscillations in the ionospheric *F*2 layer during high solar activity (HSA, September 2000 to August 2001) and low solar activity (LSA, January 2006 to December 2006) observed at SJC during different levels of geomagnetic activity. The GW/TID signatures in the *F*2 layer can be seen in the isofrequency lines of virtual height daily variations for six fixed frequencies (3, 4, 5, 6, 7, and 8 MHz) which show quasiperiodic oscillations (crests and valleys). The crests and valleys when seen in close frequencies present a phase difference (i.e., first it is observed at higher frequency then at lower frequency), indicating a downward phase velocity. These quasiperiodic oscillations induced in the virtual heights are divided into three groups as small amplitude (lower than 40 km), medium amplitude (between 40 km and 60 km), and large amplitude (greater than 60 km). The observations show that GWs/TIDs are much more pronounced at *F* layer heights during HSA than LSA and the large-amplitude GWs/TIDs are present normally only during HSA.

Citation: Klausner, V., P. R. Fagundes, Y. Sahai, C. M. Wrasse, V. G. Pillat, and F. Becker-Guedes (2009), Observations of GW/TID oscillations in the *F*2 layer at low latitude during high and low solar activity, geomagnetic quiet and disturbed periods, *J. Geophys. Res.*, *114*, A02313, doi:10.1029/2008JA013448.

1. Introduction

[2] Since the pioneering work of *Hines* [1960] related to atmospheric gravity waves at ionospheric heights, hundreds of investigators have contributed to understanding the mechanism of generation (source), propagation parameters (wavelengths, periods and velocities), and spectrum of waves. Recently, *Lastovicka* [2006] has pointed out that gravity waves (GWs) are either of ''meteorological'' origin coming from below or are of auroral origin coming quasi-horizontally during geomagnetic disturbances (see, e.g., review by *Hocke and Schlegel* [1996]) or are excited in situ for instance by the solar terminator passage [e.g., *Somsikov and Ganguly*, 1995; *Galushko et al.*, 1998] or solar eclipse [*Sauli et al.*, 2006a]. As mentioned by *Schunk and Nagy* [2000], atmospheric GWs are not global and have a localized source. The importance of GWs in the upper atmosphere and ionosphere from below is well known. The main topics related in this field of research are the relationship between the role of GWs and the momentum and energy budget and the tropospheric/meteorological sources [*Bishop et al.*, 2006; *Boska and Sauli*, 2001; *Sauli and Boska*, 2001; *Sauli et al.*, 2006b; *Fritts and Alexander*, 2003; *Medeiros et al.*, 2003, 2004; *Lastovicka*, 2006; *Vadas*, 2007; *Vadas and Fritts*, 2005, 2006]. Several investigators have studied the propagation and possible sources of GWs in the mesospheric region and a significant progress has been made to understand the role of GWs at mesospheric heights [e.g., *Medeiros et al.*, 2003, 2004; *Wrasse et al.*, 2006a, 2006b]. Also, during geomagnetically disturbed periods GWs are generated at high latitude due to Joule heating and the topic received special attention during the last several decades. These waves propagate quasi-horizontally and change the ionospheric electron density profile from high latitude to equatorial region. These GWs manifest themselves in the ionosphere and are called traveling ionospheric disturbances (TIDs) [*Buonsanto*, 1999]. During the recent past GWs/TIDs received much attention due to space weather studies as geomagnetic disturbances have adverse effects on increasingly sophisticated ground- and space-based technological systems [*Buonsanto*, 1999; *Becker-Guedes et al.*, 2004; *Lima et al.*, 2004; *Sahai et al.*, 2005].

[3] However, using different techniques, recent observations from both middle and low latitudes showed that the *F* layer can be perturbed by GWs/TIDs under geomagnetic

[1]Physics and Astronomy, Universidade do Vale do Paraíba, São José dos Campos, Brazil.

0148-0227/09/2008JA013448

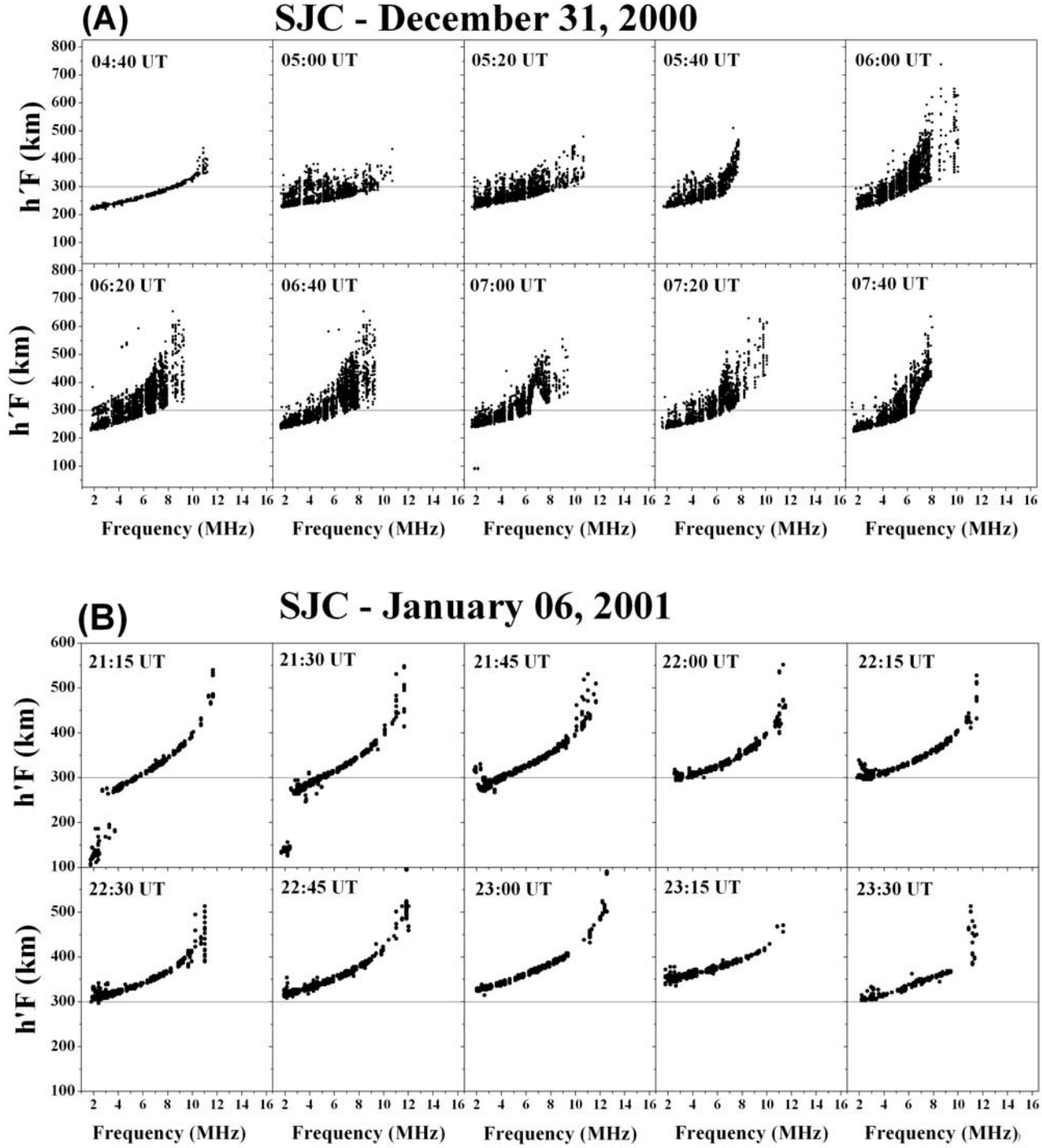

Figure 1. (a) Sequence of ionograms obtained on 31 December 2000 illustrating how the vertical profiles are severely deteriorated by the presence of spread *F*. (b) Sequence of ionograms on 6 January 2001 show the vertical displacement of the *F* layer during the prereversal peak which occurs between 2200 and 2230 UT. The black line at 300 km is used to facilitate visualizing the *F* layer vertical displacement during the prereversal peak.

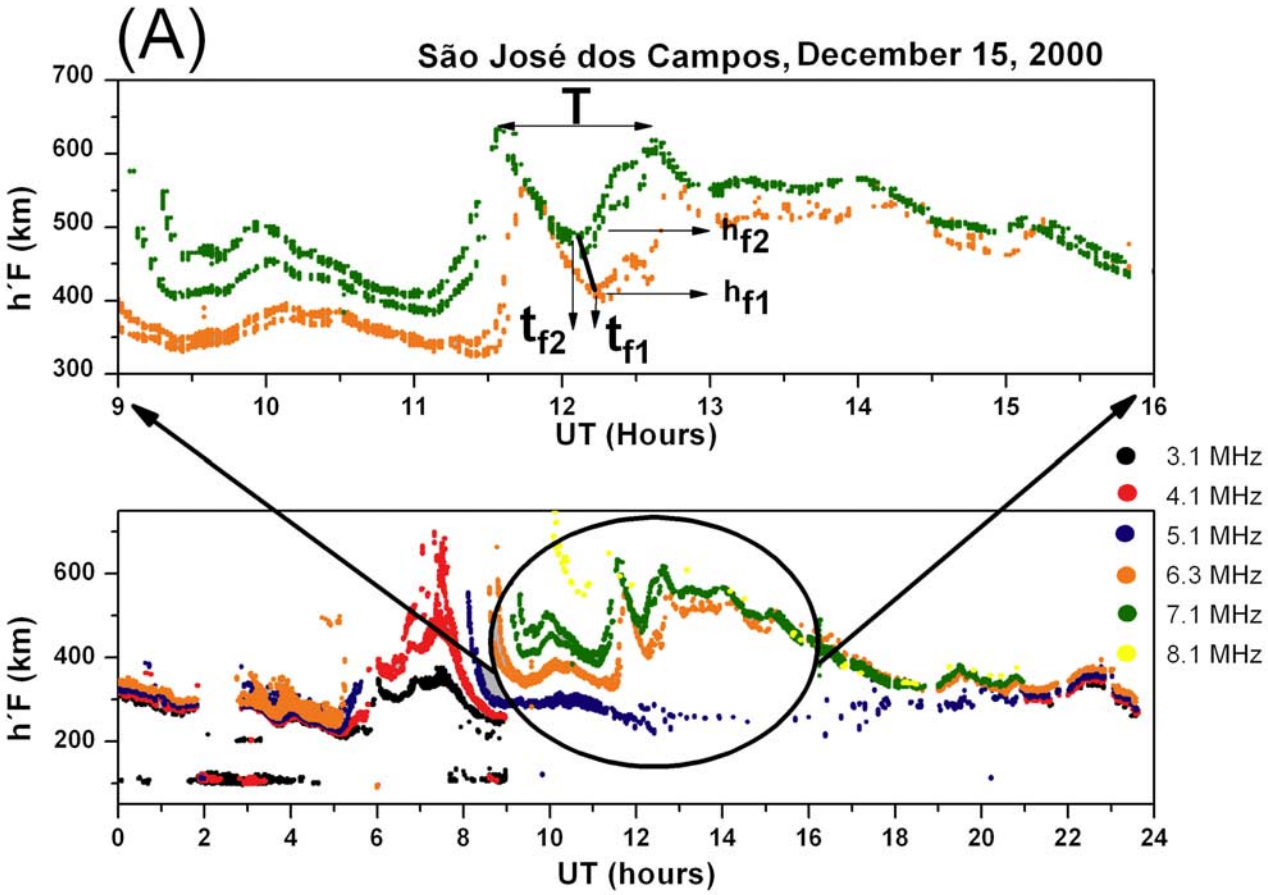

Figure 2. Daily virtual height variations for 3.1, 4.1, 5.1, 6.3, 7.1, and 8.1 MHz on 15 December 2000, 24 May 2006, and 8 June 2001. (a) On 15 December, 12 show large amplitude oscillations (greater than 60 km). Enlargement shows virtual height variations for 6.3 (orange) and 7.1 (green) MHz between 0900 and 1600 UT. Also T indicates the period of the GW, h_f is the virtual height, f1 and f2 are frequencies, and t_{f1} and t_{f2} are the time. (b) On 24 May 2006 is shown medium amplitude oscillations (between 40 km and 60 km) and (top) virtual height variations for 5 (blue) and 6 (orange) MHz between 1300 and 1800 UT. (c) On 8 June 2001 is shown small amplitude oscillations (lower than 40 km) and (top) virtual height variations for 3.1 (blue) and 5.1 (green) MHz, showing between 1300 and 2000 UT.

quiet conditions [*Boska and Sauli*, 2001; *Djuth et al.*, 2004; *Fagundes et al.*, 2007; *Galushko et al.*, 1998; *Sauli et al.*, 2006a, 2006b], from below or in situ. In fact, quasiperiodic wave like modulation in foF2 and h'F is a very common feature during geomagnetic quiet conditions. Certainly, one of the important questions is related to the sources of these GWs/TIDs and according to recent investigations there are several possible sources. The sources of GWs/TIDs at mesosphere–lower thermosphere and lower ionosphere are predominantly from below (troposphere–stratosphere). However, there are also a few studies showing the propagation of GWs due to tropospheric sources at *F* region heights [*Boska and Sauli*, 2001; *Sauli and Boska*, 2001; *Rottger*, 1977; *Fagundes et al.*, 2007]. The signature of GWs/TIDs at *F* layer heights is more complex according to *Djuth et al.* [2004]. They mention that above ~130 km, neutral motion parallel to the geomagnetic field moves the plasma up and down field lines, and at lower altitudes plasma motions are primarily determined by the wind-induced Lorentz force that acts on the ions. It is important to mention that *Vadas* [2007], using a ray trace model which incorporates a new dispersion relationship, showed that GWs from below with the same values of λ_H and λ_z typically dissipate at somewhat higher altitudes when the thermosphere is hotter. This suggests that during high solar activity the GWs activity is higher at thermospheric heights than during low solar activity.

2. Observations and Data Analysis

[4] A Canadian Advanced Digital Ionosonde (CADI) is in routine operation at Sao Jose dos Campos (23.2°S, 45.9°W; dip latitude 17.6°S, UT = LT + 3), since August 2000. The CADI is simultaneously operational in two different ways. The first one sweeps 180 frequencies from 1 to 20 MHz sampling with regular temporal resolution of 300 s (5 min) and these measurements provide normal ionograms (see Figure 1). The second one sweeps only six preselected frequencies (3.1, 4.1, 5.1, 6.3, 7.1, and 8.1 MHz were used during the period of HSA and 3, 4, 5, 6, 7, and 8 MHz were used for LSA) with a rapid sequence of soundings every 100 s and these measurements make

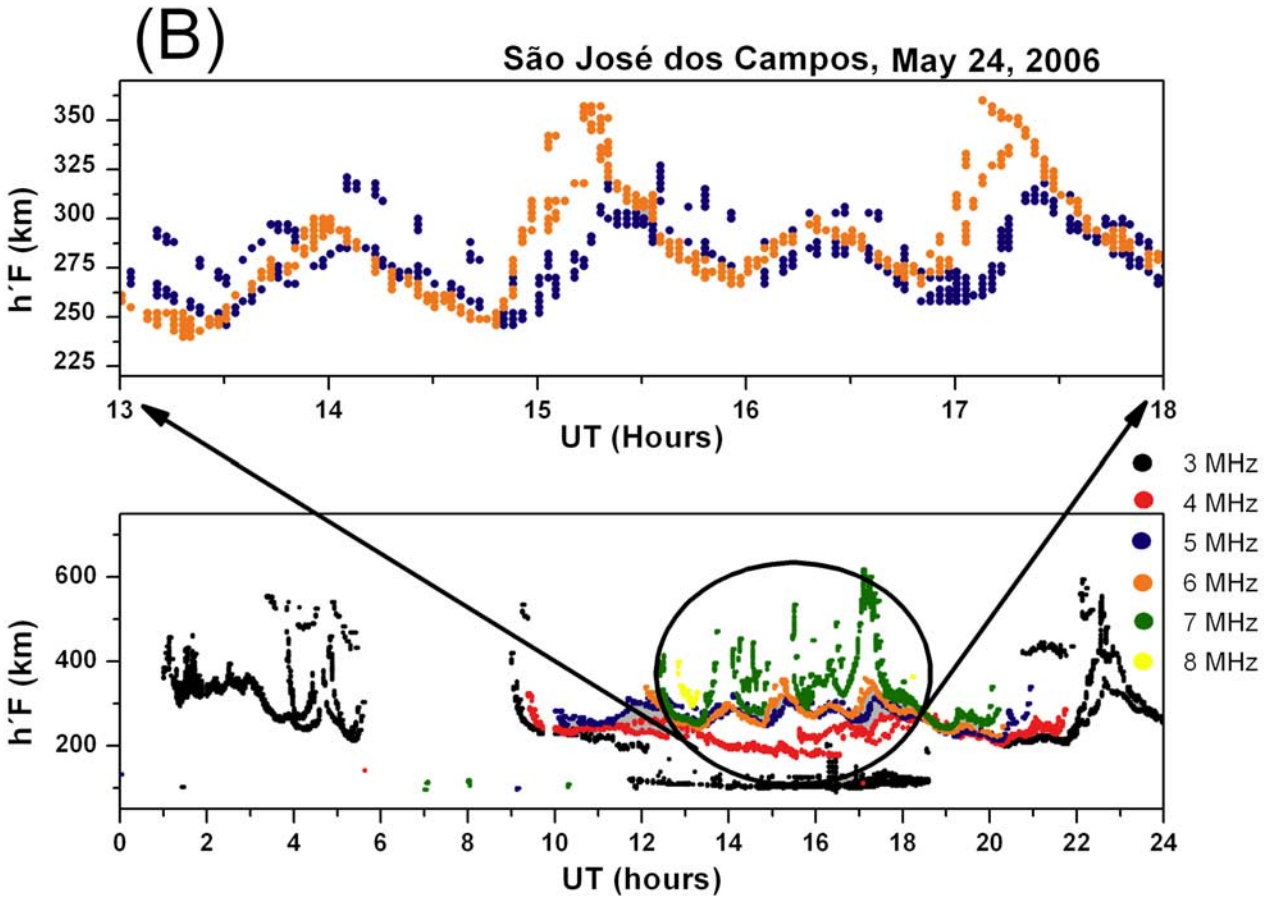

Figure 2. (continued)

possible isofrequency plots (see Figure 2). For the second survey it was decided to use integer values close to the original choice of frequencies. The systematic shift is only 0.1 MHz, and we do not believe this influences the deductions made in this study.

[5] As shown by *Fagundes et al.* [2007], it is possible to use the virtual height values extracted directly from the second mode of operation, with high rate of sampling (100 s), to investigate the daily virtual height variations for each of the six frequencies (isofrequency lines). Also, the rate of sampling of 100 s allows us to study GW/TID propagations with periods larger than 3 min (200 s). However, the periods observed are of the order of about 30 min.

[6] On many occasions, it is possible to observe wave like oscillations propagating through the *F* layer on ionograms and the parameters (T, V_z, and λ_z) of these waves agree with the GW theory. However, the quasiperiodic oscillations produced by GWs/TIDs are better detected and visualized using the virtual height daily variations at constant frequencies (isofrequency lines). Since the observed GW/TIDs periods in this study are about 30–180 min, the rate of sampling of 100 s appears to be appropriate. Then using the isofrequency lines it is possible to infer the GWs/TIDs period (T) by just calculating the time lag of two consecutive peaks or valleys for a specific frequency (i.e., first they are observed at higher frequency and then at lower frequency), showing a downward phase velocity, see Figure 2a. The vertical phase velocity (V_z) is calculated using the virtual height and time of peak/valley of two nearby frequencies

$$V_z = {}^{(h_{f2} - h_{f1})}\Big/_{(t_{f2} - t_{f1})}$$

where h is virtual height, $f2$ and $f1$ are nearby frequencies, and t is time. Finally, the vertical wavelength (λ_z) can be calculated using $\lambda_v = V_z T$ (for more details see Figure 2a). Then, the amplitude of the GW/TID is defined as the difference between successive crest and valley heights (for more details see Figure 2a).

[7] The period and vertical velocity phase mentioned above are the limitations of the instrumentation for studying GW using isofrequency plots. *Becker-Guedes et al.* [2004] and *Lima et al.* [2004] have used same isofrequency lines at two different ionospheric sounding stations to study the response of the ionospheric *F* layer during geomagnetically disturbed periods and GWs/TIDs propagating to low-latitude region.

[8] Using ionospheric sounding observations from September 2000 to August 2001 as representative of high solar activity and observations between January 2006 and December 2006 for low solar activity, we have investigated the GWs month-to-month occurrence variation and its parameters (T, V_z, and λ_z) at *F* region heights as a

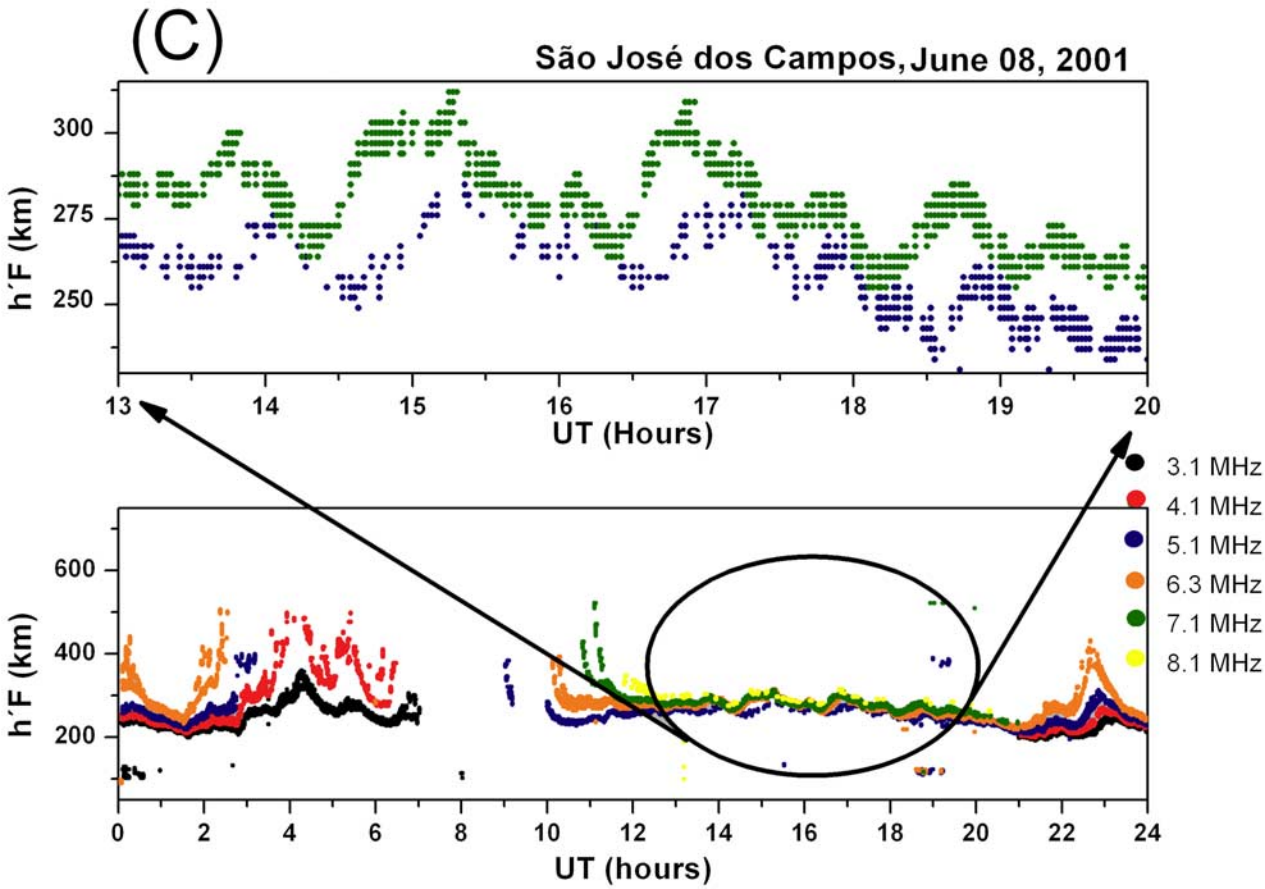

Figure 2. (continued)

function of solar activity. Both geomagnetically quiet and disturbed period data have been used.

[9] Detection of GWs/TIDs at low-latitude ionospheric heights, using ionosonde observations, is subject to several limitations since the vertical plasma density profile could be perturbed by the presence of equatorial spread *F*, electric fields, or waves (e.g., planetary, tidal, and gravity waves). Although electric fields and waves have different signatures, sometime they occur simultaneously and this makes the study of propagation GWs/TIDs at ionospheric heights very complex during geomagnetically disturbed periods. Nevertheless, with the advent of digital ionosonde with high sampling rate sometimes it is possible to distinguish between electric field and GW/TIDs effects [*Fagundes et al.*, 2007].

[10] The study of GWs/TIDs propagation at equatorial and low-latitude ionospheric heights presents another difficulty. Figure 1a shows the presence of spread *F* on ionograms on the night of 31 December 2000. Then during high spread *F* occurrence season, the study of GWs/TIDs during nighttime will be severely prejudiced. The presence of spread *F* blocks any possibility to see the quasiperiodic wave like modulation in the isofrequency lines induced by GWs/TIDs. Again, Figure 1b shows the extension to low latitude of the prereversal enhancement which takes place between late afternoon and early night in the magnetic equator region, due to the action of eastward electric field that lifts the entire *F* layer upward until it reaches a maximum virtual height around 1900–1930 LT and after that a westward electric field moves it downward. Also, the prereversal peak signature appears in Figures 2a, 2b, and 2c between 2200 UT (1900 LT) and 2400 UT (2100 LT). Therefore, to avoid complications associated with the prereversal and spread *F*, we have concentrated our studies mostly during the daytime.

[11] These quasiperiodic oscillations in virtual heights at different frequencies present amplitudes varying from about 20 to 100 km. Then, these quasiperiodic oscillations of GWs/TIDs are classified according to the amplitude of oscillations induced in virtual heights in three different groups: small amplitude (lower than 40 km), medium amplitude (between 40 km and 60 km), and large amplitude (greater than 60 km). In order to illustrate the characteristics of the large, medium, and small amplitudes of quasiperiodic oscillations a sequence of three examples is shown in Figures 2a, 2b, and 2c (bottom) during a full day of observations. Notice in Figures 2a, 2b, and 2c (top) that the amplitude of the quasiperiodic oscillations is not constant along the time.

[12] In order to study the month-to-month occurrence of GWs/TIDs at the *F* region heights as a function of solar activity, 2 years (September 2000 to August 2001 (HAS) and January 2006 to December 2006) of ionospheric data were examined for quasiperiodic oscillations due to GWs/TIDs. The total amount of hours of GWs (large, medium, and small) during HSA and LSA were 3909 h and 415 h,

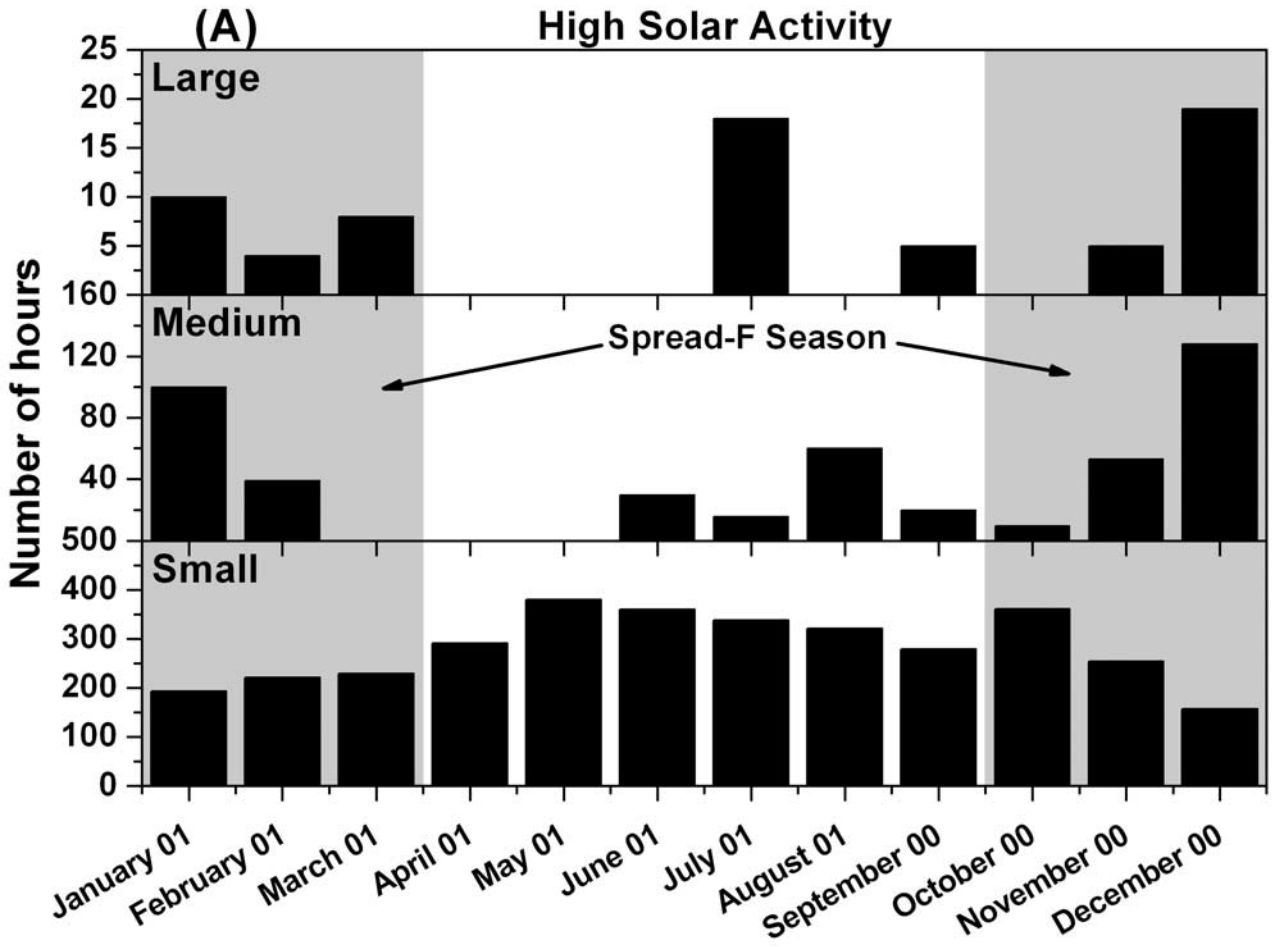

Figure 3. (a) Monthly variations of gravity wave occurrences from September 2000 to August 2001 (high solar activity) for large, medium, and small amplitude oscillations and (b) January 2006 to December 2006 (low solar activity). The gray portions indicate the high season spread *F* (January to March and October to December).

respectively. The analysis showed that GWs/TIDs are present during HSA at *F* layer heights on almost every day, but during LSA the occurrence is about 9 times less frequent than HSA.

[13] The monthly variations of these three categories of quasiperiodic oscillations in HSA and LSA induced by GWs/TIDs are shown in histograms (Figures 3a and 3b). The month-by-month numbers of hours of occurrence of these events are presented for HSA and LSA. In addition, the seasons in the South American sector are subdivided as follows: November, December, January, and February (summer); May, June, July, and August (winter); March and April (autumn equinox); and September and October (spring equinox). Figures 4a and 4b show the observed period (T) and vertical phase speed (V_z) parameters of GWs/TIDs extracted from isofrequency lines as well the calculated vertical wavelength (λ_z) parameter for both high solar and low solar activity.

[14] When the quasiperiodic amplitude oscillations are separated into three different categories very interesting results come out. It is possible to note in Figure 3a that quasiperiodic oscillations with small amplitude (<40 km) are present during HSA throughout the year with maximum occurrence frequency during the period May to August. Both autumn (March and April) and spring (September and October) showed small amplitude oscillations which are more frequent than during the summer months. A perusal of Figure 3a shows that when the occurrence of small quasiperiodic oscillations decreases (summer), then the occurrence of medium and large oscillations increases.

[15] Figure 3b shows that during LSA, all the months have occurrence of quasiperiodic oscillation, but the amount of time is about 9 times less than HSA. However, it is important to point out that the percentages of occurrence of small, medium, and large amplitude oscillations during LSA (82% small, 17% medium, and 1% large) is very similar to those during HSA (86% small, 12% medium, and 2% large). Nevertheless, there is no clear trend in seasonal variations during LSA in the quasiperiodic oscillations (small, medium, and large) as noticed during HSA. However, it is important to mention that large amplitude oscillations were observed only during December and the maximum occurrence for the medium amplitude oscillations were observed during April and May.

[16] Table 1 shows that small quasiperiodic amplitude oscillations during HSA contributed with 86% (3384 h) of

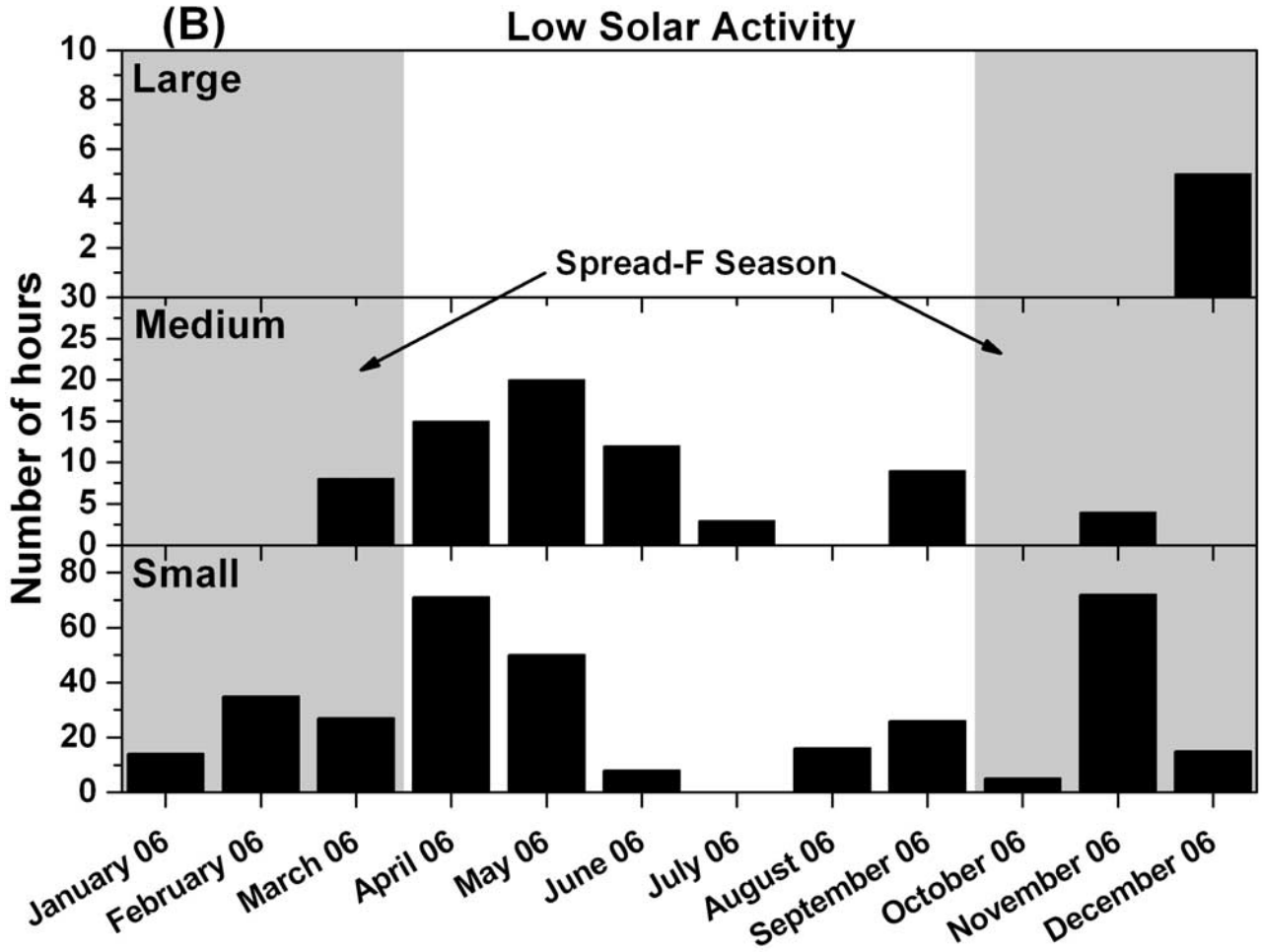

Figure 3. (continued)

the cases. On the other hand, medium amplitude oscillations contributed with 12% (456 h) and large amplitude oscillations contributed with 2% (69 h). Also, Table 1 shows that frequency of occurrence is maximum during wintertime (May, June, July, and August), with total amount of 1399 h (41%). On the other hand, a minimum in occurrence takes place during the summertime (November, December, January, and February), with a total amount of 825 h (25%). Since the number of months for each season is not the same and the smaller sample sizes during the LSA period introduces large variability, in Table 1 observation hours per month and the error have been added. Notice that during HSA the error is large only for summer months with large amplitude (4.5%). However, for LSA the error for small amplitude is large only during autumn months (2.1%). For medium amplitude during the winter, autumn, and spring months, percentage errors of 4.2%, 4.8%, and 3.0%, respectively, have been obtained. The largest percentage error for large amplitude is noted during summer months (22.4%) owing to the very small sample size.

[17] In addition, from Table 1 it is possible to notice that the quasiperiodic amplitude oscillations with medium and large amplitudes have maximum occurrence during summer solstice, with a total amount of 358 h (68%) compared with a total amount 124 h (winter, 24%), 8 h (autumn, 1%), and 35 h (spring, 7%). However, the small number of cases of large and medium oscillations does not allow a conclusive result. Also, some seasonal variations are noted when the amplitudes of oscillation are separated into small, medium, and large categories. But when we add total amount of hours (small + medium + large) for each month it is not possible to notice any seasonal variation, although March with 237 h shows minimum level and June with 390 h shows maximum level of quasiperiodic oscillations. The total amount of hours of quasi periodic amplitude oscillations (small + medium + large) for each season (Table 1) may suggest a different result, but we must remember that summer and winter have 4 months and equinox of autumn and spring have only 2 months.

[18] Figure 4 shows the observed gravity wave parameters (T, V_z, and λ_z) during high and low solar activities, under both quiet and disturbed periods. Figure 4a shows the parameters for GWs with small amplitude and Figure 4b for GWs with medium/large amplitudes. Owing to the large number of GW events during HSA it is possible to see the details in the histograms for all the parameters. However, owing to limited of number of events observed during LSA and geomagnetically disturbed periods during

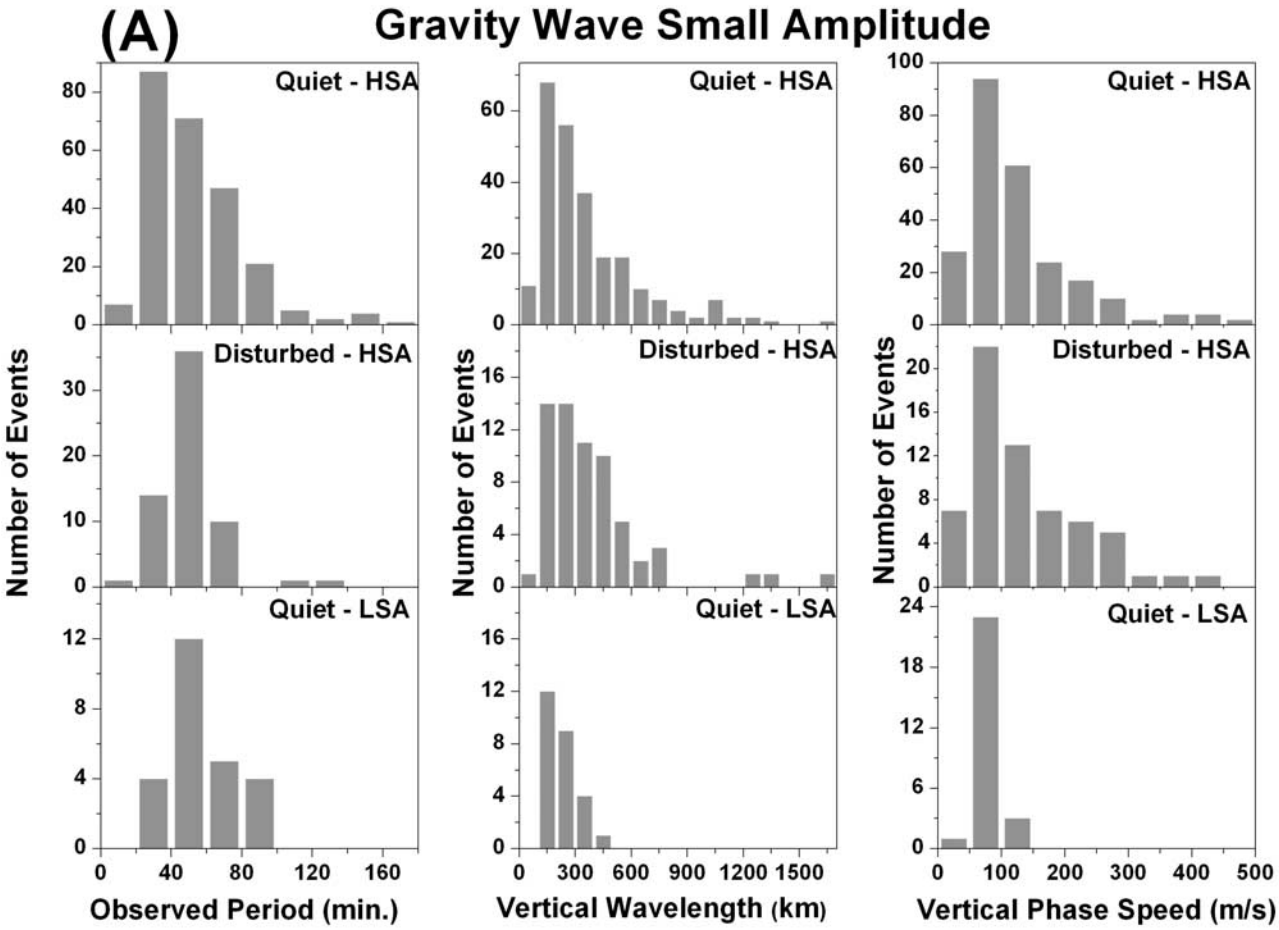

Figure 4. Gravity wave parameters obtained from the oscillations induced in the *F*2 layer virtual height. (a) The observed period, vertical wavelength, and phase speed for the small-amplitude gravity waves, measured on quiet and disturbed days during high solar activity and quiet days during low solar activity. (b) The parameters for medium/large amplitude gravity waves observed in the same period shown in Figure 4a.

HSA the GWs histograms become degraded, but important information about the GWs characteristics during LSA and geomagnetically disturbed periods during HSA can be evaluated.

[19] Figure 4a shows the observed period for small-amplitude waves distributed lie mainly between 30 and 90 min, 30 and 70 min, and 30 and 90 min during quiet (HSA), disturbed (HSA), and quiet (LSA) days, respectively. Since there are a large number of GW events during quiet time (HSA); it is possible see very clearly the frequency of occurrence in periods, wavelengths, and vertical phase velocities of the GWs. Also, the period of about 30 min has the largest occurrence with more than 80 events. However, during the disturbed time (HSA) and quiet time (LSA) the largest period is about 50 min. The vertical wavelength ranges mainly from 50 to 650 km, 150 to 450 km, and from 150 to 350 km for quiet (HSA), disturbed (HSA), and quiet (LSA) days, respectively. However, during quiet and disturbed (HSA) day some waves with vertical wavelength greater than 900 km are also observed. It is important to mention that in all cases the wavelength of 150 km has the maximum occurrence. For the vertical phase speed, the waves showed velocities ranging from 25 to 225 m/s, between 25 and 225 m/s, and around 75 m/s during quiet (HSA), disturbed (HSA) days, and quiet (LSA) days, respectively. In quiet and disturbed (HSA) days it is also noticed some events with vertical phase speed larger than 250 m/s. The phase velocity of about 175 m/s has the maximum occurrence in all three studied periods (quiet-HSA, disturbed-HSA, and quiet-LSA).

[20] Figure 4b shows the observed period for medium/large amplitude quasiperiodic oscillations which are distributed mainly between 30 and 110 min, between 30 to 90 min, and between 50 to 130 min during quiet (HSA), disturbed (HSA), and quiet (LSA) days, respectively. The observed GWs with medium/large amplitudes (quiet-HSA) presented maximum occurrence period of about 30–50 min., whereas for the disturbed (HSA) and quiet (LSA), the maximum occurrence period is about 50 min and 70–90 min, respectively. The vertical wavelength during quiet-HSA ranges mainly from 50 to 950 km with a maximum of about 250 km. The vertical wavelength during disturbed-HSA

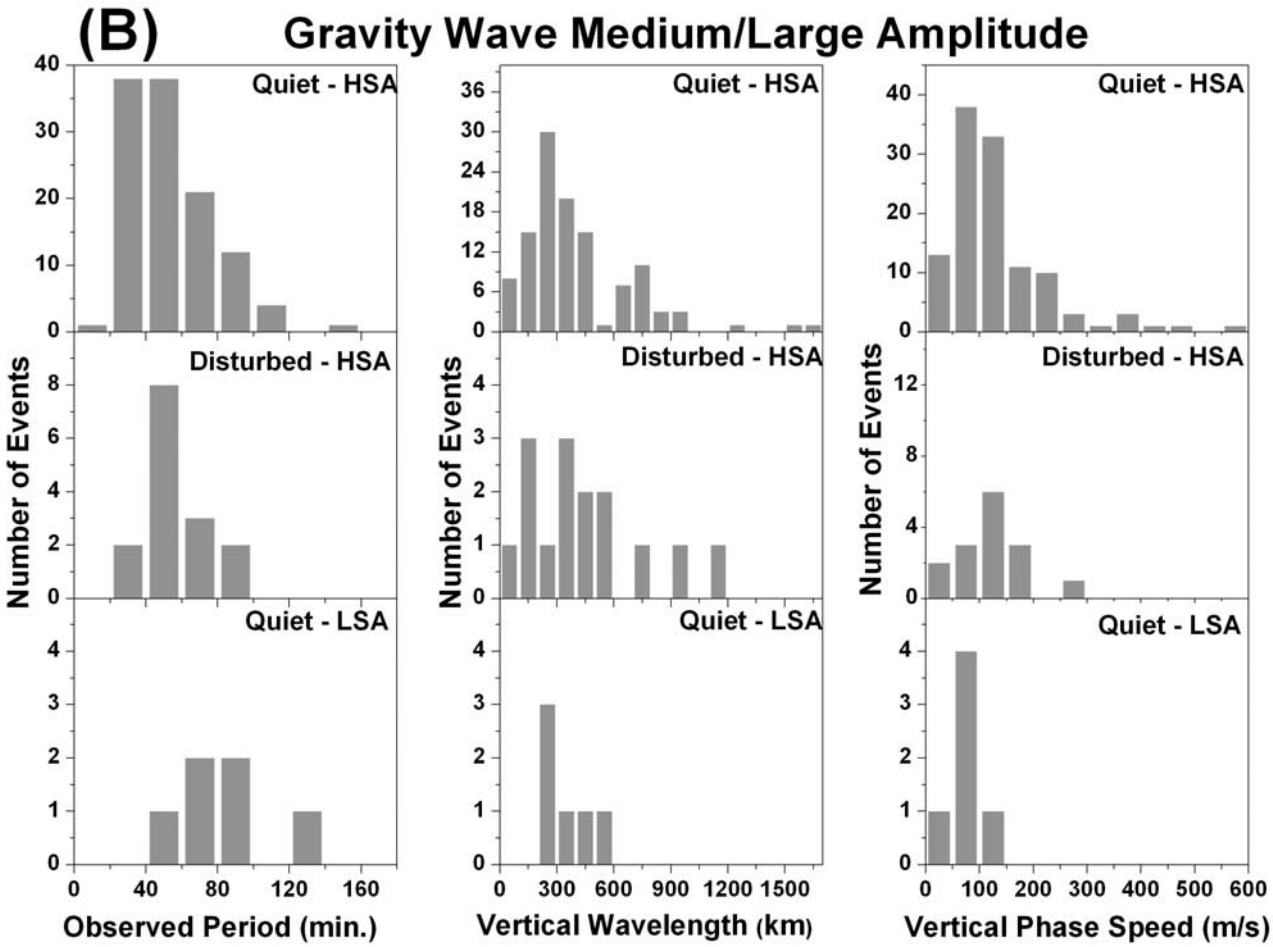

Figure 4. (continued)

spreads out from about 50 to 1150 km with maxima occurrence at about 150 and 350 km. The vertical wavelength during quiet-LSA has maximum occurrence at about 250 km. However, during quiet and disturbed (HSA) days some quasiperiodic oscillations showed vertical wavelength greater than 900 km, which was not observed during quiet (LSA) days.

[21] For the vertical phase speed, the waves showed velocities ranging from 25 to 275 m/s, around 125 m/s, and around 75 m/s during quiet (HSA), disturbed (HSA), and quiet (LSA) days, respectively. In quiet (HSA) days, some waves with vertical phase speed larger than 250 m/s are observed. Notice that small-amplitude GW parameters for quiet and disturbed periods during HSA have fairly similar maximum in occurrences in periods, vertical wavelengths, and vertical phase velocities. However, for medium/large amplitudes the quiet-HSA and disturbed-HSA presents different maximum in occurrences.

3. Discussion

[22] The mesosphere and lower thermosphere (upper atmosphere) are strongly affected by propagation of GWs with period of minutes to hours. These waves may alter significantly the momentum, energy budget, and wind system of the upper atmosphere [*Lastovicka*, 2006; *Fritts and Alexander*, 2003]. Up to now the study of propagation and possibly sources of GWs at mesosphere region have been the subject of a number of papers and significant progress has been made to understand the role of GWs at mesospheric heights [*Medeiros et al.*, 2003, 2004; *Wrasse et al.*, 2006a, 2006b]. In addition, GWs associated with geomagnetic storms at the ionosphere–thermosphere heights are well studied. These waves originate in auroral regions and propagate to low latitudes quasi-horizontally. These waves have a well-defined source and induce quasi-periodic oscillations in the ionosphere at *F* layer heights and are commonly called traveling ionospheric disturbances (TIDs).

[23] The wide spectrum of GW amplitudes (small, medium, and large) found in this investigation may be related to the wave breaking process. GWs with large and medium amplitudes may break into GWs with small amplitude at lower altitude (upper mesosphere or lower thermosphere) and these secondary waves can penetrate to the ionospheric *F* layer heights. *Vadas and Fritts* [2002] carried out a theoretical study and conclude that secondary waves may be able to escape the shears in the upper mesosphere and

Table 1. Details of the Total Number of Hours for Each Category of Amplitude During a Full Year[a]

	Total Year (h)	Summer (h)	Winter (h)	Autumn (h)	Spring (h)
Small/HSA	3384 (86%)	825 (25%)	1399 (41%)	520 (15%)	640 (19%)
Hours/month (error)		206 (0.004)	350 (0.006)	260 (0.005)	320 (0,005)
Medium/HSA	456 (12%)	320 (70%)	106 (23%)	0 (0%)	30 (7%)
Hours/month (error)		80 (0.020)	27 (0.010)	0 (0.000)	15 (0.008)
Large/HSA	69 (2%)	38 (55%)	18 (26%)	8 (12%)	5 (7%)
Hours/month (error)		10 (0.050)	5 (0.007)	4 (0.004)	3 (0.005)
Total of hours (HSA)	3909 (100%)	1183 (30%)	1523 (39%)	528 (14%)	675 (17%)
Small/LSA	339 (82%)	136 (40%)	74 (22%)	98 (29%)	31 (9%)
Hours/month (error)		34 (0.017)	19 (0.013)	49 (0.021)	16 (0.012)
Medium/LSA	71 (17%)	4 (6%)	35 (49%)	23 (32%)	9 (13%)
Hours/month (error)		1 (0.014)	9 (0.042)	12 (0.048)	5 (0.030)
Large/LSA	5 (1%)	5 (100%)	0 (0%)	0 (0%)	0 (0%)
Hours/month (error)		1 (0.224)	0 (0.000)	0 (0.000)	0 (0.000)
Total of hours (LSA)	415 (100%)	145 (35%)	109 (26%)	121 (29%)	40 (10%)

[a]Categories of amplitude are small, medium, and large. Full year consists of summer (4 months), winter (4 months), autumn (2 months), and spring (2 months). Error is given by $\left(\sqrt{\frac{N}{m}}\Big/ N_{Total}\right)$, where N is the number of hours in the season, m is the number of months, and N_{Total} is the total number of hours during the year.

penetrate well into lower thermosphere. This may explain the large occurrence of small-amplitude GWs.

[24] On the other hand, the study of GWs at thermosphere and ionosphere heights, with sources from below and in situ, needs more attention, because GWs are also observed during quiet time at *F* layer heights and the sources for waves during geomagnetic quiet time is not very well established as yet. Meteorological/tropospheric sources have been proposed by a number of researchers [e.g., *Boska and Sauli*, 2001; *Djuth et al.*, 2004; *Rottger*, 1977; *Sauli and Boska*, 2001]. A recent theoretical work by *Vadas and Fritts* [2005, 2006] show that GWs from convective sources in the troposphere can propagate well into the thermosphere before dissipating, and the momentum flux divergence which occurs where GWs dissipate in the thermosphere is likely to results in the excitation of large-scale TIDs and medium-scale TIDs and the creation of neutral winds. Also, *Vadas* [2007] showed that when the thermosphere is hotter the GWs dissipate at somewhat higher altitudes than when the thermosphere is cooler. This may explain our results that showed that during LSA the occurrence of GWs is about 9 times less frequent than HSA. It is important to mention that SJC is under the equatorial anomaly crest and the electron densities during LSA are large enough to carry out the gravity wave studies. The number of gravity waves observed at LSA is not limited by poor signal, i.e., it is not an instrumental effect. However, it is important to mention that *Lastovicka* [2001] has reported at midlatitude the GWs activity decreases from the solar maximum to the solar cycle minimum by about 1/3, which possibly is associated with the in situ sources.

[25] In this investigation we show that the *F* layer is modulated by quasiperiodic oscillations due to GWs during daytime. However, GWs activity is 9 times larger during HSA than during LSA. This suggests that the solar flux density is in some way related with the source(s) of the GWs at the *F* layer heights. However, in situ GW excitations should be at lower *F* layer heights (bottomside of *F*1 layer $\sim$150–170 km), due to the observed downward phase propagation, as showed in Figures 2a and 2c, which indicates that the energy propagates upward [*Hines*, 1960]. In Figure 2b the downward phase propagation is not clear, probably because there are two or more waves superimposed. On the other hand, the present results reinforce *Vadas* [2007] results showing that GWs penetrate into higher altitudes during the HSA. In order to investigate the possible sources (in situ or from below) of GWs at ionospheric *F* region heights, it will be important to carry out multi-instrument and multisite campaigns using ionosondes, GPS, optical instruments, radar, and also model simulation.

4. Summary

[26] Ionospheric sounding observations during HSA (September 2000 to August 2001) and LSA (January 2006 to December 2006), have been carried out at SJC (23°S), Brazil, and the objective of this paper is to study the propagation of GWs at *F* layer heights as a function of solar cycle and geomagnetic activity. The main results are summarized below:

[27] 1. At low latitude, Brazilian sector, GWs propagate through *F* layer heights during both HSA and LSA, but the occurrence of GWs during HSA is about 9 times larger than during LSA.

[28] 2. There is a strong relationship between the GWs activity and solar activity. This reinforces the proposal from model simulations that larger temperatures during HSA allow GWs to penetrate into higher altitudes.

[29] 3. During HSA the observed small quasiperiodic amplitude oscillations (lower than 40 km) due to GWs propagation at *F* layer heights present a maximum occurrence during wintertime and minimum during summertime.

[30] 4. Medium amplitude oscillations (between 40 km and 60 km) and large amplitude oscillations (greater than 60 km) during HSA have maximum occurrence during summertime.

[31] 5. Small, medium, and large quasiperiodic oscillations do not present clear seasonal variations during LSA.

[32] **Acknowledgments.** Amitava Bhattacharjee thanks Amauri Medeiros and another reviewer for their assistance in evaluating this paper.

References

Becker-Guedes, F., Y. Sahai, P. R. Fagundes, W. L. C. Lima, V. G. Pillat, J. R. Abalde, and J. A. Bittencourt (2004), Geomagnetic storm and equatorial spread-F, *Ann. Geophys.*, *22*, 3231–3239.

Bishop, R. L., N. Aponte, G. D. Earle, M. Sulzer, M. F. Larsen, and G. S. Peng (2006), Arecibo observations of ionospheric perturbations associated with the passage of Tropical Storm Odette, *J. Geophys. Res.*, *111*, A11320, doi:10.1029/2006JA011668.

Boska, J., and P. Sauli (2001), Observations of gravity waves of meteorological origin in the *F* region ionosphere, *Phys. Chem. Earth*, *26*(6), 425–428.

Buonsanto, M. J. (1999), Ionospheric storms - A review, *Space Sci. Rev.*, *88*(3/4), 563–601, doi:10.1023/A:1005107532631.

Djuth, F. T., M. P. Sulzer, S. A. Gonzales, J. D. Mathews, J. H. Elder, and R. L. Walterscheid (2004), A continuum of gravity waves in the Arecibo thermosphere?, *Geophys. Res. Lett.*, *31*, L16801, doi:10.1029/2003GL019376.

Fagundes, P. R., V. Klausner, Y. Sahai, V. G. Pillat, F. Becker-Guedes, F. C. P. Bertoni, M. J. A. Bolzan, and J. R. Abalde (2007), Observations of daytime *F*2-layer stratification under the southern crest of the equatorial ionization anomaly region, *J. Geophys. Res.*, *112*, A04302, doi:10.1029/2006JA011888.

Fritts, D. C., and M. J. Alexander (2003), Gravity wave dynamics and effects in the middle atmosphere, *Rev. Geophys.*, *41*(1), 1003, doi:10.1029/2001RG000106.

Galushko, V. G., V. V. Paznukhov, Y. M. Yampolski, and J. C. Foster (1998), Incoherent scatter radar observations of AGW/TID events generated by the moving solar terminator, *Ann. Geophys.*, *16*, 821–827, doi:10.1007/s00585-998-0821-3.

Hines, C. O. (1960), Internal atmospheric gravity waves at ionospheric heights, *Can. J. Phys.*, *38*, 1441–1481.

Hocke, K., and K. Schlegel (1996), A review of atmospheric gravity waves and traveling ionospheric disturbances: 1982–1995, *Ann. Geophys.*, *14*(9), 917–940.

Lastovicka, J. (2001), Effects of gravity and planetary waves on the lower ionosphere as obtained from radio wave absorption measurements, *Phys. Chem. Earth*, *26*(6), 381–386.

Lastovicka, J. (2006), Forcing of the ionosphere by waves from below, *J. Atmos. Sol. Terr. Phys.*, *68*(3–5), 479–497, doi:10.1016/j.jastp.2005.01.018.

Lima, W. L. C., F. Becker-Guedes, Y. Sahai, P. R. Fagundes, J. R. Abalde, G. Crowley, and J. A. Bittencourt (2004), Response of the equatorial and low-latitude ionosphere during the space weather events of April 2002, *Ann. Geophys.*, *22*, 3211–3219.

Medeiros, A. F., M. J. Taylor, H. Takahashi, P. P. Batista, and D. Gobbi (2003), An investigation of gravity wave activity in the low-latitude upper mesosphere: Propagation direction and wind filtering, *J. Geophys. Res.*, *108*(D14), 4411, doi:10.1029/2002JD002593.

Medeiros, A. F., R. A. Buriti, E. A. Machado, H. Takahashi, P. P. Batista, D. Gobbi, and M. J. Taylor (2004), Comparison of gravity wave activity observed by airglow imaging at two different latitudes in Brazil, *J. Atmos. Sol. Terr. Phys.*, *66*(6–9), 647–654, doi:10.1016/j.jastp.2004.01.016.

Rottger, J. (1977), Travelling disturbances in the equatorial ionosphere and their association with penetrative cumulus convection, *J. Atmos. Terr. Phys.*, *39*, 987–998, doi:10.1016/0021-9169(77)90007-1.

Sahai, Y., et al. (2005), Effects of the major geomagnetic storms of October 2003 on the equatorial and low-latitude *F* region in two longitudinal sectors, *J. Geophys. Res.*, *110*, A12S91, doi:10.1029/2004JA010999.

Sauli, P., and J. Boska (2001), Tropospheric events and possible related gravity wave activity effects on the ionosphere, *J. Atmos. Sol. Terr. Phys.*, *63*(9), 945–950.

Sauli, P., P. Abry, J. Boska, and L. Duchayne (2006a), Wavelet characterisation of ionospheric acoustic and gravity waves occurring during the solar eclipse of August 11, 1999, *J. Atmos. Sol. Terr. Phys.*, *68*(3–5), 586–598, doi:10.1016/j.jastp.2005.03.024.

Sauli, P., P. Abry, D. Altadill, and J. Boska (2006b), Detection of the wave-like structures in the F region electron density: Two station measurements, *Stud. Geophys. Geod.*, *50*(1), 131–146, doi:10.1007/s11200-006-0007-y.

Schunk, R. W., and A. F. Nagy (2000), *Ionospheres: Physics, Plasma Physics, and Chemistry*, 274 pp., Cambridge Univ. Press, New York.

Somsikov, V. M., and B. Ganguly (1995), On the formation of atmospheric inhomogeneities in the solar terminator region, *J. Atmos. Terr. Phys.*, *57*(12), 1513–1523, doi:10.1016/0021-9169(95)00014-S.

Vadas, S. L. (2007), Horizontal and vertical propagation and dissipation of gravity waves in the thermosphere from lower atmospheric and thermospheric sources, *J. Geophys. Res.*, *112*, A06305, doi:10.1029/2006JA011845.

Vadas, S. L., and D. C. Fritts (2002), The importance of spatial variability in the generation of secondary gravity waves from local body forces, *Geophys. Res. Lett.*, *29*(20), 1984, doi:10.1029/2002GL015574.

Vadas, S. L., and D. C. Fritts (2005), Thermospheric responses to gravity waves: Influences of increasing viscosity and thermal diffusivity, *J. Geophys. Res.*, *110*, D15103, doi:10.1029/2004JD005574.

Vadas, S. L., and D. C. Fritts (2006), Influence of solar variability on gravity wave structure and dissipation in the thermosphere from tropospheric convection, *J. Geophys. Res.*, *111*, A10S12, doi:10.1029/2005JA011510.

Wrasse, C. M., et al. (2006a), Reverse ray tracing of the mesospheric gravity waves observed at 23 degrees S (Brazil) and 7 degrees S (Indonesia) in airglow imagers, *J. Atmos. Sol. Terr. Phys.*, *68*(2), 163–181, doi:10.1016/j.jastp.2005.10.012.

Wrasse, C. M., et al. (2006b), Mesospheric gravity waves observed near equatorial and low-middle latitude stations: Wave characteristics and reverse ray tracing results, *Ann. Geophys.*, *24*(12), 3229–3240.

F. Becker-Guedes, P. R. Fagundes, V. Klausner, V. G. Pillat, Y. Sahai, and C. M. Wrasse, Physics and Astronomy, Universidade do Vale do Paraíba, Avenida Shishima Hifumi, 2911 São José dos Campos, SP, Brazil. (fagundes@univap.br)